Collisional effects in gas lasers

Ashish Agarwal and R. Ghosh
School of Physical Sciences, Jawaharlal Nehru University, New Delhi 110 067, India
(Received 9 July 1992; revised manuscript received 14 October 1992)

The effects of phase-interrupting and velocity-changing collisions between active and perturber atoms on the spectral profile of a gas laser are studied. Exact analytical results for the density matrix are presented for the case of strong collisions in a unidirectional ring laser, and the laser intensity is then evaluated in the Doppler limit under the condition of self-consistency. The washout of the hole burning in the steady-state population difference and the broadening of the laser line shape are discussed. The results of the third-order perturbation theory are compared with the exact calculations valid for an arbitrarily intense pump.

PACS number(s): 42.55.−f, 34.10.+x, 42.60.Jf

I. INTRODUCTION

For the past 25 years or so, the effect of collisions on spectroscopic line shapes of atomic and molecular vapors has invited the attention of researchers in the field [1,2]. Recently, the effects of collisions on nonlinear mixing signal line shapes have also been investigated [3]. In order to explain the observed line shapes of these systems, it was found necessary to include atomic collisions in the theory.

In the case of gas lasers, the lasing atoms are not stationary and the field appears Doppler shifted in frequency to the atoms resulting in inhomogeneous broadening. The existing theories of gas lasers [4,5] do not take into account the effect of atomic collisions in a microscopic way. Assuming that the atoms have a Maxwellian (Gaussian) velocity distribution, the laser spectrum in the absence of collisions is given by a Voigt profile, which is the convolution of the Gaussian and a Lorentzian associated with each velocity subclass of atoms. There have been quite a few attempts [6] to modify Lamb's theory [4] to include gas-collision effects and fit experimental data of collision-broadened linewidth, but with not much success. Collisions of active atoms with buffer atoms can result in changes in the velocity of active atoms in addition to being phase interrupting (dephasing) in their effect on level coherences (off-diagonal elements of the density matrix of the system under consideration). It is known that elastic and inelastic collisions, which only perturb the phase or amplitude of an oscillating atom without changing its velocity, lead to homogeneous line broadening and a shift of its line center. The collision-induced modification of the velocity associated with the atomic state coherence may, however, become significant and affect the line shape when the collision time (given by the ratio of the mean free path and the average speed of active atoms) is much shorter compared with the interaction time (lifetime of the excited level) with the radiation field. Thus these effects show up at high perturber pressures or when the lifetime of the active atoms is long (i.e., the natural width of the laser line is small).

In this paper, we incorporate these collisional mechanisms following the scheme of Berman [1,3], and develop a self-consistent microscopic theory of the gas laser. For simplicity, we consider the case of a single-mode unidirectional ring laser, but the results can be readily generalized to the standing-wave and multimode cases. In Sec. II, we present a scheme for calculation of the density-matrix elements of the active atoms, undergoing collisions with perturber atoms, in the presence of a single-mode electric field in a unidirectional ring laser cavity. The field-atom interaction is written in the rotating-wave approximation (RWA) and the collisions are treated in the impact approximation. In Sec. III, using the strong-collision model, an exact analytical solution for the steady-state density matrix is obtained. In Sec. IV, the steady-state population difference is calculated in the Doppler limit. In the absence of velocity-changing collisions (VCC's), the plot of the population difference versus atomic velocity shows "hole burning" as usual, but VCC's are shown to cause a washout of the holes. In Sec. V, the macroscopic polarization induced in the medium is calculated as a sum of the individual atomic dipole moments, and then inserted into the self-consistency equation to yield a single-mode amplitude-determining equation. In Sec. V A, the laser threshold condition and the tuning dependence of the intensity are calculated using third-order perturbation theory, valid for low excitations (weak pumps). In Sec. V B, the problem is treated nonperturbatively and the intensity spectral profile is calculated for arbitrarily high excitations. Deviations from the third-order predictions are pointed out. Finally, we summarize the results in Sec. VI.

II. COLLISIONAL MODEL IN A GAS LASER

In order to illustrate the basic laser principles, it suffices to consider an active medium consisting of two-level atoms interacting with a single longitudinal mode of a scalar, plane-wave electric field in a one-dimensional resonant cavity of length L (say, along the z direction).

The electric field in the laser cavity can be written as

$$\mathcal{E}(z,t)=\tfrac{1}{2}E(t)\exp\{-i[\nu t+\phi(t)]\}U(z)+\text{c.c.} \quad (2.1)$$

Here the mode amplitude $E(t)$ and phase $\phi(t)$ vary little in an optical period, and $(\nu+\dot{\phi})$ is the mode frequency. $U(z)$ is the normal-mode function. For the two-mirror laser, it is the standing wave,

$$U(z)=\sin(Kz) , \tag{2.2}$$

and for the unidirectional ring laser, it is the running wave,

$$U(z)=\exp(iKz) , \tag{2.3}$$

with wave vector K. With Eq. (2.1) for the field, the induced polarization of the medium can be written in the form

$$\mathcal{P}(z,t)=\tfrac{1}{2}P(t)\exp[-i(\nu t+\phi)]U(z)+\text{c.c.} , \tag{2.4}$$

where $P(t)$ is a complex, slowly varying component of the polarization. The real part of $P(t)$ is in phase with the electric field and results in dispersion due to the medium. The imaginary part is in quadrature with the electric field and results in gain or loss.

In the standard model [4] of a gas laser, the laser medium consists of two-level atoms (upper level a, lower level b) interacting with a radiation field. The levels a and b, separated by an optical frequency ω, are assumed to be of opposite parity. Each level is incoherently pumped at some rate $\lambda_i(z,v,t)$ from outside the two-level atom subspace, and owing to spontaneous emission, each level decays at a rate γ_i, where $i=a,b$. An atom at time t and position z and with z component of velocity v is described by the density matrix $\rho(z,v,t)$.

Neglecting collisions, the time evolution of the active atom density matrix $\rho(z,v,t)$ is given by the master or transport equation [4],

$$\dot{\rho}=-i\hbar^{-1}[\mathcal{H},\rho]-\tfrac{1}{2}(\Upsilon\rho+\rho\Upsilon)+\Lambda , \tag{2.5}$$

where matrix elements of the Hamiltonian $\mathcal{H}$ are given by

$$\mathcal{H}_{ij}=\varepsilon_i\delta_{ij}-\mu_{ij}\mathcal{E}(z,t)(1-\delta_{ij}) , \tag{2.6}$$

and the decay operator Υ and the excitation matrix Λ have the elements

$$\Upsilon_{ij}=\gamma_i\delta_{ij} , \tag{2.7}$$

$$\Lambda_{ij}=\lambda_i\delta_{ij} , \tag{2.8}$$

where $i,j=a,b$; ε_i is the energy of level i and μ_{ij} is the dipole-matrix element between states i and j, assumed to be real and equal to μ.

The active or emitter atoms (i.e., those atoms that interact strongly with the external radiation field) of the gas undergo collisions with perturber or buffer atoms (i.e., atoms for which the radiation field is far off resonance). The density of active atoms is assumed to be sufficiently low so that collisions between two active atoms are neglected. The atomic transition frequency ω is shifted by Kv as a result of atomic motion. Collisions with perturber atoms can cause a shift in velocity v besides interrupting the phase of the oscillating dipoles. The limiting case of a state-independent collision interaction might occur if a and b are two levels within the same electronic state, with ω corresponding to a fine structure, vibration, or rotation transition. For a state-independent collision interaction, collisions result solely in a change of velocity of the active atom, with no instantaneous change in phase for the dipoles.

The active atom-perturber atom collisions are treated in the impact approximation. In this approximation, the duration of a typical collision τ_c is assumed to be much less than the various time scales in the problem, with the exception of the optical period, i.e., τ_c^{-1} is much greater than the atom-field detuning, Rabi frequency, and collisional decay rates. Changes in velocity v occur through jumps from the value of v to another value. The jump time is assumed to be instantaneous with respect to all other relevant time scales in the problem. Moreover, we make the Markov approximation, so that the value of v following a jump depends at most on its value before the jump. We further assume the statistical independence of velocity-changing and phase-interrupting collisions.

Each collision produces a change in the density matrix associated with the active atoms. The change produced by the field during the collisions is assumed to be negligible. With these approximations, the net effect of collisions is the addition of a term $[\partial\rho(z,v,t)/\partial t]_{\text{coll}}$ to the right-hand side of Eq. (2.5). Explicitly, the collisional contribution is found to be [1]

$$\left[\frac{\partial}{\partial t}\rho_{ij}(z,v,t)\right]_{\text{coll}} = -\gamma_p(v)(1-\delta_{ij})\rho_{ij}(z,v,t)-\Gamma_{ij}(v)\rho_{ij}(z,v,t) + \int dv' W_{ij}(v'\to v)\rho_{ij}(z,v',t) . \tag{2.9}$$

The quantity $\gamma_p(v)$ is the decay rate corresponding to phase-interrupting collisions; it vanishes for $i=j$. The quantity $W_{ii}(v'\to v)$ is a collision kernel giving the probability density per unit time that a collision changes the velocity of an active atom in state i from v' to v. Changes in v occur at some average rate $\Gamma_{ij}(v)$, which is related to the kernel in the following way:

$$\Gamma_{ij}(v)=\int dv' W_{ij}(v\to v') . \tag{2.10}$$

Thus the second term on the right-hand side in Eq. (2.9) can be viewed as the "out term" resulting from collisions that remove active atoms in state i from the velocity subclass v, and the last term is the "in term" bringing atoms from other velocity subclasses into the subclass v. W_{ii} is related to the differential scattering cross section and Γ_{ii} is related to the corresponding total scattering cross section.

For the case of the unidirectional running wave laser with the mode function given by Eq. (2.3), we introduce an interaction representation in which

$$\rho_{ab}(z,v,t)=\mathcal{N}\tilde{\rho}_{ab}(v,t)\exp\{i[Kz-\nu t-\phi(t)]\} =[\rho_{ba}(z,v,t)]^* , \tag{2.11a}$$

$$\rho_{ii}(z,v,t)=\mathcal{N}\rho_{ii}(v,t), \quad i=a,b , \tag{2.11b}$$

where $\mathcal{N}$ is the active atom density, and thereby eliminate

the optical frequency variations of the off-diagonal elements of the density matrix. Using Eqs. (2.5) and (2.9), we find that the density-matrix elements evolve as

$$\frac{d}{dt}\tilde{\rho}_{ab}(v,t)=-[\gamma+\gamma_p(v)+\Gamma_{ab}(v)+i\Omega(v)]\tilde{\rho}_{ab}(v,t) +i\chi(t)[\rho_{aa}(v,t)-\rho_{bb}(v,t)] +\int dv' W_{ab}(v'\to v)\tilde{\rho}_{ab}(v',t) , \tag{2.12a}$$

$$\frac{d}{dt}\rho_{aa}(v,t)=\lambda_a(v,t)-[\gamma_a+\Gamma_{aa}(v)]\rho_{aa}(v,t) +i[\chi(t)\tilde{\rho}^*_{ab}(v,t)-\chi^*(t)\tilde{\rho}_{ab}(v,t)] +\int dv' W_{aa}(v'\to v)\rho_{aa}(v',t) , \tag{2.12b}$$

$$\frac{d}{dt}\rho_{bb}(v,t)=\lambda_b(v,t)-[\gamma_b+\Gamma_{bb}(v)]\rho_{bb}(v,t) -i[\chi(t)\tilde{\rho}^*_{ab}(v,t)-\chi^*(t)\tilde{\rho}_{ab}(v,t)] +\int dv' W_{bb}(v'\to v)\rho_{bb}(v',t) , \tag{2.12c}$$

where we have assumed a spatially uniform excitation mechanism such that

$$\lambda_i(z,v,t)=\mathcal{N}\lambda_i(v,t), \quad i=a,b \tag{2.13a}$$

and

$$\Omega(v)\equiv Kv+\omega-\nu-\dot{\phi} , \tag{2.13b}$$

and χ is the Rabi frequency given by

$$\chi(t)=\frac{\mu E(t)}{2\hbar} \tag{2.13c}$$

and

$$\gamma=\tfrac{1}{2}(\gamma_a+\gamma_b) . \tag{2.13d}$$

In the above equations, the perturbation energy [second term on the right-hand side in Eq. (2.6)] has been written in the rotating-wave approximation [4(a)].

The solution of Eqs. (2.12) for an arbitrary collision kernel can be obtained through extensive numerical computation. In the steady state, from Eq. (2.12a), the solution for the off-diagonal element can be written as [1]

$$\tilde{\rho}_{ab}(v)=-i\chi\int_{-\infty}^{\infty}dv'\int_0^{\infty}dt\,\exp[-\{\gamma+\gamma_p+i(\omega-\nu)\}t]G_{ab}(v'\to v,t)[\rho_{aa}(v')-\rho_{bb}(v')] , \tag{2.14}$$

where the propagator $G_{ab}(v'\to v,t)$ satisfies

$$\frac{\partial G_{ab}(v'\to v,t)}{\partial t}=iKvG_{ab}(v'\to v,t)-\Gamma_{ab}(v)G_{ab}(v'\to v,t)+\int_{-\infty}^{\infty}dv''W_{ab}(v''\to v)G_{ab}(v'\to v'',t) , \tag{2.15a}$$

subject to the initial condition

$$G_{ab}(v'\to v,0)=\delta(v-v') . \tag{2.15b}$$

The iterative solution to Eq. (2.15) is

$$G_{ab}(v'\to v,t)=\exp[-\Gamma_{ab}(v')t]\exp(iKv't)\delta(v-v') +\int_0^t dt'\exp[-\Gamma_{ab}(v')t']\exp(iKv't')W_{ab}(v'\to v)\exp[-\Gamma_{ab}(v)(t-t')]\exp[iKv(t-t')]+\cdots . \tag{2.16}$$

III. RESULTS IN THE STRONG COLLISION MODEL

Exact analytical solutions of Eqs. (2.12) can be worked out for various limiting forms of the collision kernel. Of particular interest is the so-called strong-collision model. The model is especially suited if the mass of the perturber atoms is much larger than the mass of the active atoms. A single collision, on average, thermalizes the velocity distribution. The collision kernel is then given by

$$W_{ij}(v'\to v)=\Gamma_{ij}(v)M(v) , \tag{3.1}$$

where $M(v)$ is the Maxwellian velocity distribution given by

$$M(v)=(\sqrt{\pi}u)^{-1}\exp[-(v/u)^2] , \tag{3.2}$$

with u being the most probable speed. We can further neglect the velocity dependence of $\gamma_p(v)$ and $\Gamma_{ij}(v)$ without much error because they are generally slowly varying functions of v. Equations (2.12) for density-matrix elements can then be recast in a compact form,

$$\frac{d}{dt}\psi(v,t)=-A(v,t)\psi(v,t) +BM(v)\int\psi(v',t)dv'+C(v,t) , \tag{3.3}$$

where

$$\psi(v,t)=\begin{bmatrix}\tilde{\rho}_{ab}(v,t)\\ \tilde{\rho}^*_{ab}(v,t)\\ \rho_{aa}(v,t)-\rho_{bb}(v,t)\\ \rho_{aa}(v,t)+\rho_{bb}(v,t)\end{bmatrix} , \tag{3.4a}$$

$$A(v,t)=\begin{bmatrix}\Gamma_0+i\Omega(v) & 0 & i\chi(t) & 0\\ 0 & \Gamma_0-i\Omega(v) & -i\chi^*(t) & 0\\ 2i\chi^*(t) & -2i\chi(t) & a & b\\ 0 & 0 & b & a\end{bmatrix} , \tag{3.4b}$$

and nonvanishing elements of B and $C(v,t)$ are given by

$$B_{11}=B_{22}=\Gamma_{ab},\quad B_{33}=B_{44}=\tfrac{1}{2}(\Gamma_{aa}+\Gamma_{bb}),$$
$$B_{34}=B_{43}=\tfrac{1}{2}(\Gamma_{aa}-\Gamma_{bb}), \tag{3.4c}$$
$$C_{31}=\lambda_a(v,t)-\lambda_b(v,t),\quad C_{41}=\lambda_a(v,t)+\lambda_b(v,t), \tag{3.4d}$$
$$\Gamma_0=\gamma+\gamma_p+\Gamma_{ab}, \tag{3.4e}$$

and

$$a=\tfrac{1}{2}(\gamma_a+\gamma_b+\Gamma_{aa}+\Gamma_{bb}),$$
$$b=\tfrac{1}{2}(\gamma_a-\gamma_b+\Gamma_{aa}-\Gamma_{bb}). \tag{3.4f}$$

We are interested in the steady-state behavior of the laser system. The steady-state solution for ψ can be obtained by setting the left-hand side of Eq. (3.3) equal to zero. This yields the exact analytical solution for the density matrix,

$$\psi(v)=A^{-1}(v)BM(v)[\mathcal{I}-\int dv''M(v'')A^{-1}(v'')B]^{-1}\times\int dv'A^{-1}(v')C(v')+A^{-1}(v)C(v), \tag{3.5}$$

where $\mathcal{I}$ is a unit matrix of dimension (4×4) and $A(v)$ and $C(v)$ are steady-state values of $A(v,t)$ and $C(v,t)$, respectively.

IV. CALCULATION OF POPULATION DIFFERENCE IN DOPPLER LIMIT

It is almost impossible to calculate the polarization and the intensity in its exact form using (3.5). One may use the relatively simple and often applicable Doppler limit in which the Doppler width Ku is much larger than the homogeneous decay constant γ, collisional parameters, and the Rabi frequency. Let χ be the steady-state value of Rabi frequency $\chi(t)$, and $\lambda_a(v)$ and $\lambda_b(v)$ the steady-state values of the excitation rates $\lambda_a(v,t)$ and $\lambda_b(v,t)$, respectively. We further assume a pumping mechanism which factors as

$$\lambda_i(v)=\lambda_i M(v),\quad i=a,b, \tag{4.1}$$

for which the velocity distribution $M(v)$ is Maxwellian (3.2) with most probable speed u. Integrals in the above expression for $\psi(v)$ can be reduced to the form $\int dv\,M(v)[v^2+\Omega(v)^2]^{-1}$, where

$$v=\Gamma_0\left[1+\frac{2\chi^2}{R_s\Gamma_0}\right]^{1/2} \tag{4.2}$$

is the "power-broadened" total decay constant, and

$$\frac{1}{R_s}=\frac{1}{\gamma_a+\Gamma_{aa}}+\frac{1}{\gamma_b+\Gamma_{bb}}. \tag{4.3}$$

This integral can be written in terms of the plasma dispersion function [4(a)] as

$$\int dv\,M(v)[v^2+\Omega(v)^2]^{-1}=(Kuv)^{-1}Z_i(v+i(\omega-\nu)), \tag{4.4}$$

where Z_i is the imaginary part of plasma dispersion function Z. In the Doppler limit

$$\left|\frac{v}{Ku}\right|\ll 1, \tag{4.5}$$

integral (4.4) reduces to [4(a)]

$$\int dv\,M(v)[v^2+\Omega(v)^2]^{-1}\cong\frac{\sqrt{\pi}}{Kuv}\exp\left[-\left[\frac{\omega-\nu}{Ku}\right]^2\right]. \tag{4.6}$$

Also it is assumed that the perturber pressure is low enough so that $\Gamma_{ab}\ll Ku$, and the terms with Γ_{ab}/Ku dependence can be ignored in the expression for $\psi(v)$. With these approximations, the formal expression for the steady-state value of $\tilde{\rho}_{ab}$ is obtained from Eq. (3.5) as

$$\tilde{\rho}_{ab}(v)=-i\chi[\rho_{aa}(v)-\rho_{bb}(v)]\mathcal{D}(\Omega(v)), \tag{4.7}$$

where we have used the notation $\mathcal{D}(\Omega)$ for a complex Lorentzian,

$$\mathcal{D}(\Omega)=1/(\Gamma_0+i\Omega). \tag{4.8}$$

The steady-state population difference is

$$\rho_{aa}(v)-\rho_{bb}(v)=\frac{NM(v)}{S[1+R(v)/R_s]}, \tag{4.9}$$

where the unsaturated population difference is

$$N=\lambda_a\gamma_a^{-1}-\lambda_b\gamma_b^{-1}, \tag{4.10}$$

the rate constant is

$$R(v)=\frac{2\chi^2}{\Gamma_0}\mathcal{L}(\Omega(v)), \tag{4.11}$$

the dimensionless Lorentzian $\mathcal{L}(\Omega)$ is

$$\mathcal{L}(\Omega)=\frac{\Gamma_0^2}{\Gamma_0^2+\Omega^2}, \tag{4.12}$$

and the scaling factor due to VCC's is

$$S=1+\frac{2\sqrt{\pi}}{Ku}\chi^2\left[1+\frac{2\chi^2}{R_s\Gamma_0}\right]^{-1/2}\times\left[\frac{\Gamma_{aa}/\gamma_a}{(\gamma_a+\Gamma_{aa})}+\frac{\Gamma_{bb}/\gamma_b}{(\gamma_b+\Gamma_{bb})}\right]\times\exp\left[-\left[\frac{\omega-\nu}{Ku}\right]^2\right]. \tag{4.13}$$

In the absence of field, $R(v)=0$ and $S=1$, and so the population difference is $NM(v)$. In the absence of collisions, to the lowest order in χ, the spectrum is a Voigt profile, i.e., the convolution of a Gaussian of width Ku and a Lorentzian of width 2γ,

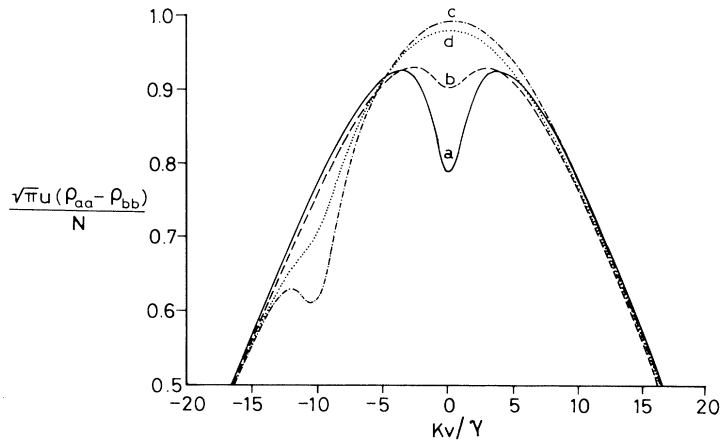

FIG. 1. Plots of the steady-state saturated population difference $\rho_{aa}-\rho_{bb}$ [in the units of $(\sqrt{\pi}u)^{-1}N$] vs velocity v (in the units of γ/K) [Eq. (4.9)]; curve a, on resonance ($\omega=\nu$), without VCC's ($\Gamma_{ab}=0$); curve b, on resonance ($\omega=\nu$), with moderate VCC parameters ($\Gamma_{ab}=0.5\gamma$); curve c, off resonance ($\omega-\nu=10\gamma$), without VCC's ($\Gamma_{ab}=0$); curve d, off resonance ($\omega-\nu=10\gamma$), with moderate VCC parameters ($\Gamma_{ab}=0.5\gamma$). We have made the choice $\Gamma_{aa}=3\Gamma_{ab}$, $\Gamma_{bb}=\Gamma_{ab}$; decay rates $\gamma_a=0.6\gamma$, $\gamma_b=1.4\gamma$, collisional dephasing parameter $\gamma_p=0.6\gamma$, Doppler width $Ku=20\gamma$, and Rabi frequency $\chi=0.3\gamma$.

$$\tilde{\rho}_{ab}=\int dv\,\tilde{\rho}_{ab}(v)\simeq\frac{-i\chi N}{\gamma}\int dv\,M(v)\gamma^2/[\gamma^2+\Omega(v)^2] \tag{4.14}$$

to first order in χ, where the Lorentzian absorption profile [(4.12) with $\Gamma_0\to\gamma$] associated with each velocity subclass of atoms is weighted by the Gaussian distribution $M(v)$ of (3.2). Collisions modify the line shape in two ways. First, there is a broadening and shifting of the line because of γ_p. Second, there is a collision-induced modification of the velocity associated with the atomic state coherence $\tilde{\rho}_{ab}$ which becomes significant at high pressures. Figure 1 shows the plots of the steady-state population difference $\rho_{aa}-\rho_{bb}$ [Eq. (4.9)] versus velocity v on and off resonance, with and without VCC's. As expected, the Lorentzian (4.12) in (4.9) gives rise to hole burning in the absence of VCC's. The Lorentzian is peaked at the detuning value $\omega-\nu=-Kv$, i.e., a hole is burned at $v=(\nu-\omega)/K=c(1-\omega/\nu)$, where c is the velocity of light, as shown in Fig. 1, curve a (on resonance) and curve c (off resonance). But the VCC's tend to wash out the hole burning (Fig. 1, curves b and d). This is in qualitative agreement with the computed and experimental findings of Smith [[6(b)], Fig. 3]. The washout of the hole burning can be explained by the process of cross relaxation between atoms of different velocity groups. As collisions change the atomic velocity without inducing transitions, the burnt hole gets spread over the entire velocity distribution.

V. CALCULATION OF INTENSITY PROFILE

The macroscopic polarization $\mathcal{P}(z,t)$ induced in the laser medium is contributed by all atoms regardless of their velocity and is given by [4]

$$\mathcal{P}(z,t)=\mu\int dv\,\rho_{ab}(z,v,t)+\text{c.c.}\ , \tag{5.1}$$

where the evolution of the population matrix $\rho_{ab}(z,v,t)$ is given by Eqs. (2.5) and (2.9). Comparing Eq. (5.1) with Eq. (2.4) and using the transformation (2.11a), we get the complex polarization

$$P(t)=2\mathcal{N}\mu\int dv\,\tilde{\rho}_{ab}(v,t)\ . \tag{5.2}$$

Substituting the value of $\tilde{\rho}_{ab}(v)$ from Eq. (4.7), and using (4.9), we find the complex polarization in the steady state as

$$P=-\frac{2i\mu\mathcal{N}N\chi}{S}\int dv\frac{M(v)\mathcal{D}(\Omega(v))}{[1+R(v)/R_s]}\ . \tag{5.3}$$

The above integral can be evaluated using again the plasma dispersion function in the Doppler limit (4.5) and using the result (4.6). We find that

$$P=-\frac{2i\sqrt{\pi}\mu\mathcal{N}N\chi}{KuS}\left[1+\frac{2\chi^2}{R_s\Gamma_0}\right]^{1/2}\times\exp\left[-\left[\frac{\omega-\nu}{Ku}\right]^2\right]\ . \tag{5.4}$$

In a laser, the field has to obey the condition of self consistency; that is, the electric field that induces polarization in the gain medium should be equal to the one supported by that gain in the cavity. This leads to the following self-consistency equation for the mode amplitude [4]:

$$\dot{E}+\frac{\nu}{2Q}E=-\frac{\nu}{2\epsilon_0}\text{Im}(P)\ , \tag{5.5}$$

where Q is the laser cavity quality factor and ϵ_0 is the permittivity of vacuum. Combining the complex polarization (5.4) with the self-consistency equation (5.5) in the steady state, we have the single-mode amplitude-determining equation

$$E\left[\frac{\sqrt{\pi}\mu^2\mathcal{N}N\nu}{2\epsilon_0\hbar KuS}\left[1+\frac{\mu^2E^2}{2\hbar^2R_s\Gamma_0}\right]^{-1/2}\times\exp\left[-\left[\frac{\omega-\nu}{Ku}\right]^2\right]-\frac{\nu}{2Q}\right]=0\ . \tag{5.6}$$

A. Third-order perturbation results

In the perturbation-theory approach, valid for weak excitations only, S in the denominator on the left-hand side of Eq. (5.6) is expanded to third order in E for calculation of the steady-state intensity. Making the approximations

$$\frac{2\chi^2}{R_s\Gamma_0}\ll 1 \tag{5.7a}$$

and

$$\frac{2\sqrt{\pi}}{Ku}R_s\Gamma_0\left[\frac{\Gamma_{aa}/\gamma_a}{(\gamma_a+\Gamma_{aa})}+\frac{\Gamma_{bb}/\gamma_b}{(\gamma_b+\Gamma_{bb})}\right]\le 1\ , \tag{5.7b}$$

we can write the steady-state amplitude-determining equation (5.6) as

$$E(\alpha-\beta I)=0\ , \tag{5.8}$$

where I is the dimensionless intensity,

$$I\equiv\frac{\mu^2E^2}{2\hbar^2\gamma_a\gamma_b}\ , \tag{5.9}$$

α is the linear net gain coefficient,

$$\alpha=\frac{\sqrt{\pi}\mu^2\mathcal{N}N\nu}{2\epsilon_0\hbar Ku}\exp\left[-\left[\frac{\omega-\nu}{Ku}\right]^2\right]-\frac{\nu}{2Q}\ , \tag{5.10}$$

and β is the self-saturation coefficient,

$$\beta=\frac{\sqrt{\pi}\mu^2\mathcal{N}N\nu}{2\epsilon_0\hbar Ku}\exp\left[-\left[\frac{\omega-\nu}{Ku}\right]^2\right]\times\left\{\frac{\gamma_a\gamma_b}{2R_s\Gamma_0}+\frac{\sqrt{\pi}}{Ku}\left[\frac{\gamma_b\Gamma_{aa}}{\gamma_a+\Gamma_{aa}}+\frac{\gamma_a\Gamma_{bb}}{\gamma_b+\Gamma_{bb}}\right]\times\exp\left[-\left[\frac{\omega-\nu}{Ku}\right]^2\right]\right\}\ . \tag{5.11}$$

Setting the linear gain coefficient $\alpha=0$ in Eq. (5.10), we determine the threshold condition (at resonance),

$$\frac{\sqrt{\pi}\mu^2\mathcal{N}}{\epsilon_0\hbar Ku}N_T=\frac{1}{Q}\ , \tag{5.12}$$

where N_T is the value of the unsaturated population difference N at threshold. This can be used to express the coefficients α and β defined by (5.10) and (5.11) in terms of the relative excitation

$$\mathfrak{N}\equiv\frac{N}{N_T}=\frac{\sqrt{\pi}\mu^2\mathcal{N}NQ}{\epsilon_0\hbar Ku}\ , \tag{5.13}$$

which is more easily measured than the excitation N. From Eq. (5.8), we get the steady-state solution for the intensity in the third-order perturbation theory,

$$I=\frac{\alpha}{\beta}=\frac{1-\exp\left[\left[\frac{\omega-\nu}{Ku}\right]^2\right]\mathfrak{N}^{-1}}{\frac{\gamma_a\gamma_b}{2R_s\Gamma_0}+\frac{\sqrt{\pi}}{Ku}\left[\frac{\gamma_b\Gamma_{aa}}{\gamma_a+\Gamma_{aa}}+\frac{\gamma_a\Gamma_{bb}}{\gamma_b+\Gamma_{bb}}\right]\exp\left[-\left[\frac{\omega-\nu}{Ku}\right]^2\right]}\ . \tag{5.14}$$

As in traditional pressure-broadening theories, if collision-induced changes in active atoms' velocities are neglected, the third-order intensity profile reduces to the known result [4(a)] for a unidirectional ring laser,

$$I=\frac{1-\exp[(\omega-\nu)^2/(Ku)^2]\mathfrak{N}^{-1}}{\gamma/(\gamma+\gamma_p)}\ . \tag{5.15}$$

Figure 2 gives the plots of the third-order intensity I as a function of detuning $(\omega-\nu)$ in the absence of VCC's [Eq. (5.15)] for various values of the excitation $\mathfrak{N}$ slightly above threshold, with moderate collisional dephasing parameter γ_p. As expected, laser intensity and linewidth increase with increasing excitation. Figure 3 shows the effect of increasing VCC parameters on intensity I of (5.14). Curve a of Fig. 3 is the same as curve d of Fig. 2. The width of the intensity profile and the intensity maximum increase with increasing VCC parameters while the excitation is kept fixed. It is evident that the line shape of the laser under combined velocity and phase modulations is not a simple Voigt convolution of the line shapes due to spontaneous decay and the velocity distribution of atoms.

B. Exact results

In the following, an exact solution for the intensity is obtained by multiplying Eq. (5.6) by S, defined in Eq. (4.13), and squaring, which yields

$$I(\alpha'-\beta' I+\vartheta I^2)=0\ , \tag{5.16}$$

where α' is the modified net gain coefficient,

$$\alpha'=\mathfrak{N}^2-\exp\left[2\left[\frac{\omega-\nu}{Ku}\right]^2\right]\ , \tag{5.17}$$

β' is the modified self-saturation coefficient,

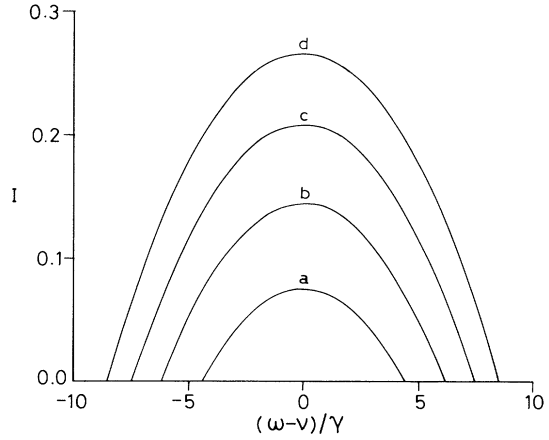

FIG. 2. Third-order intensity I as a function of detuning $(\omega-\nu)$ [Eq. (5.15)] in the absence of VCC's ($\Gamma_{aa}=\Gamma_{bb}=\Gamma_{ab}=0$), for various values of the excitation $\mathfrak{N}$ slightly above threshold: curve a, $\mathfrak{N}=1.05$; curve b, $\mathfrak{N}=1.10$; curve c, $\mathfrak{N}=1.15$; curve d, $\mathfrak{N}=1.20$. Decay constants $\gamma_a=0.6\gamma$, $\gamma_b=1.4\gamma$, collisional dephasing parameter $\gamma_p=0.6\gamma$, and Doppler width $Ku=20\gamma$.

$$\beta'=\frac{\gamma_a\gamma_b}{2R_s\Gamma_0}\exp\left[2\left[\frac{\omega-\nu}{Ku}\right]^2\right]+2\sqrt{\vartheta}\mathfrak{N}\ , \tag{5.18}$$

and ϑ is the nonlinear coefficient, with $\beta'^2\geq 4\alpha'\vartheta$,

$$\vartheta=\frac{\pi}{(Ku)^2}\left[\frac{\gamma_b\Gamma_{aa}}{\gamma_a+\Gamma_{aa}}+\frac{\gamma_a\Gamma_{bb}}{\gamma_b+\Gamma_{bb}}\right]^2 . \tag{5.19}$$

The solution of Eq. (5.16) gives the steady-state intensity as

$$I=(2\vartheta)^{-1}[\beta'-(\beta'^2-4\alpha'\vartheta)^{1/2}] . \tag{5.20}$$

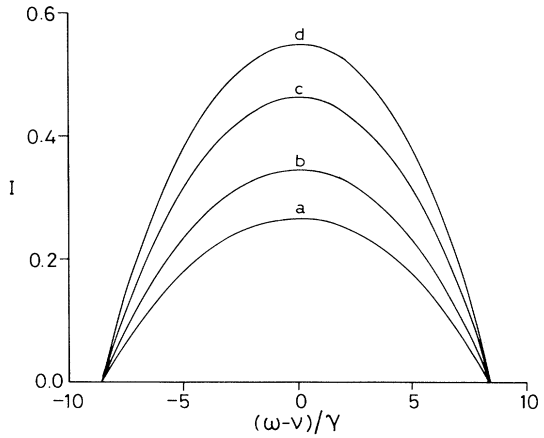

FIG. 3. Effect of increasing VCC parameters on third-order intensity I [Eq. (5.14)] for curve a, $\Gamma_{ab}=0$; curve b, $\Gamma_{ab}=0.1\gamma$; curve c, $\Gamma_{ab}=0.3\gamma$; curve d, $\Gamma_{ab}=0.5\gamma$, with $\Gamma_{aa}=3\Gamma_{ab}$, $\Gamma_{bb}=\Gamma_{ab}$. Decay rates $\gamma_a=0.6\gamma$, $\gamma_b=1.4\gamma$, collisional dephasing parameter $\gamma_p=0.6\gamma$, Doppler width $Ku=20\gamma$, and excitation $\mathfrak{N}=1.2$.

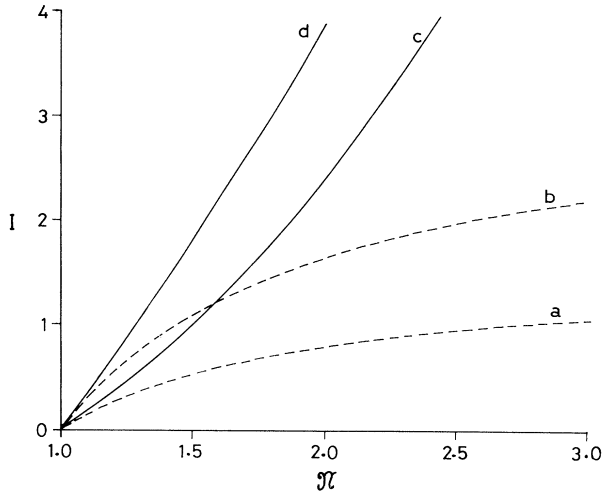

FIG. 4. Plots of the steady-state intensity I vs relative excitation $\mathfrak{N}$ near threshold at resonance ($\omega=\nu$): (i) third-order result (dashed line) curve a, without VCC's ($\Gamma_{ab}=0$) [Eq. (5.15)], curve b, with moderate VCC parameters ($\Gamma_{ab}=0.5\gamma$) [Eq. (5.14)]; (ii) exact result (solid line) curve c, without VCC's ($\Gamma_{ab}=0$) [Eq. (5.21)], curve d, with moderate VCC parameters ($\Gamma_{ab}=0.5\gamma$) [Eq. (5.20)]. Here $\Gamma_{aa}=3\Gamma_{ab}$, $\Gamma_{bb}=\Gamma_{ab}$; decay rates $\gamma_a=0.6\gamma$, $\gamma_b=1.4\gamma$, collisional dephasing parameter $\gamma_p=0.6\gamma$, and Doppler width $Ku=20\gamma$.

We have discarded the other root, $(2\vartheta)^{-1}[\beta'+(\beta'^2-4\alpha'\vartheta)^{1/2}]$ of Eq. (5.16), since it does not satisfy the threshold criterion, $I=0$ for $\alpha'=0$. If collision-induced changes in active atoms' velocities are neglected, intensity profile reduces to the known result [[4(b)] Chap. 6] for a unidirectional ring laser,

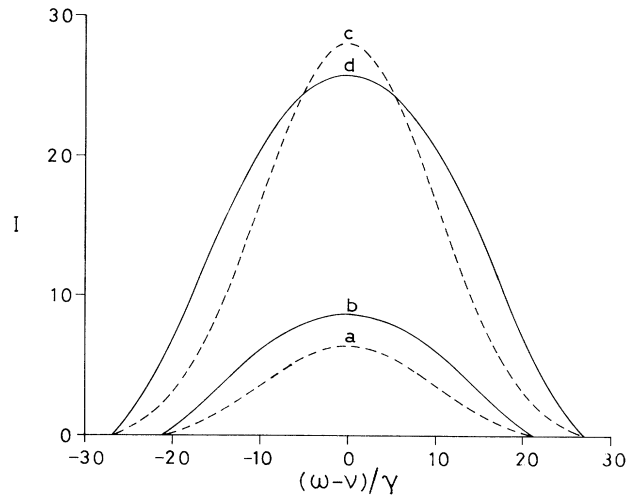

FIG. 5. Effect of increasing VCC parameters on intensity I [Eq. (5.20)] for (i) excitation $\mathfrak{N}=3$; curve a, $\Gamma_{ab}=0$ (dashed line); curve b, $\Gamma_{ab}=0.5\gamma$ (solid line); (ii) excitation $\mathfrak{N}=6$; curve c, $\Gamma_{ab}=0$ (dashed line); curve d, $\Gamma_{ab}=0.5\gamma$ (solid line). Here $\Gamma_{aa}=3\Gamma_{ab}$, $\Gamma_{bb}=\Gamma_{ab}$, decay rates $\gamma_a=0.6\gamma$, $\gamma_b=1.4\gamma$, collisional dephasing parameter $\gamma_p=0.6\gamma$, and Doppler width $Ku=20\gamma$.

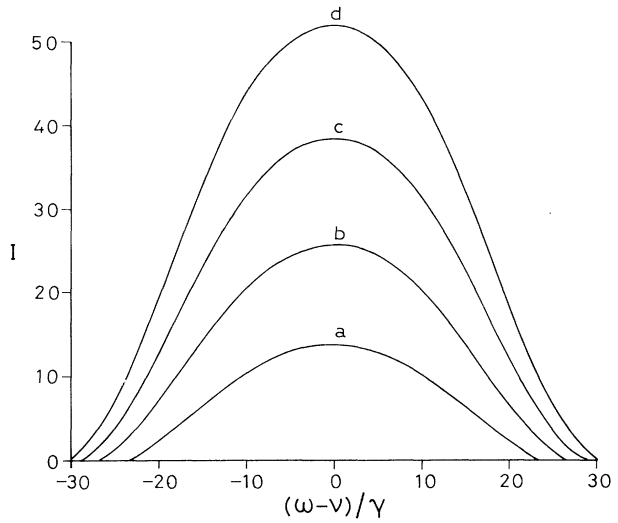

FIG. 6. Intensity I as a function of detuning $(\omega-\nu)$ [Eq. (5.20)] with moderate VCC parameters ($\Gamma_{ab}=0.5\gamma$, $\Gamma_{aa}=3\Gamma_{ab}$, $\Gamma_{bb}=\Gamma_{ab}$), for various values of the excitation $\mathfrak{N}$ well above threshold: curve a, $\mathfrak{N}=4$; curve b, $\mathfrak{N}=6$; curve c, $\mathfrak{N}=8$; curve d, $\mathfrak{N}=10$. Decay constants $\gamma_a=0.6\gamma$, $\gamma_b=1.4\gamma$, collisional dephasing parameter $\gamma_p=0.6\gamma$, and Doppler width $Ku=20\gamma$.

$$I=\frac{\mathfrak{N}^2\exp[-2(\omega-\nu)^2/(Ku)^2]-1}{\gamma/(\gamma+\gamma_p)} . \tag{5.21}$$

Figure 4 shows the plots of steady-state laser intensity I versus excitation $\mathfrak{N}$ near threshold, with and without VCC's, and compares the perturbation-theory result [Eq. (5.14)] with the exact result (5.20). As is known [5], for large $\mathfrak{N}$, intensity I of (5.14) saturates to a value (viz., $1+\gamma_p/\gamma$ in the absence of VCC's), rather than increasing with $\mathfrak{N}$. The third-order theory over-estimates the saturation and is shown here to differ from the exact result for $\mathfrak{N}\gtrsim 1.1$. Figure 5 shows the effect of increasing VCC parameters on intensity I of (5.20). The width of the intensity profile increases with increasing VCC parameters while the excitation is kept fixed at two values ($\mathfrak{N}=3$ and 6) above threshold. It is seen that at lower values of excitation $\mathfrak{N}$, the intensity maximum (at $\omega=\nu$) slowly increases with increasing VCC parameters, whereas at higher values of $\mathfrak{N}$ ($\gtrsim 5$), the peak value is reduced with increase in Γ_{ab}. Figure 6 gives the plots of intensity I of (5.20) as a function of detuning $(\omega-\nu)$ with moderate VCC parameters for various values of the excitation $\mathfrak{N}$ much above threshold, in presence of moderate collisional dephasing parameter γ_p. Curve b of Fig. 6 is the same as curve d of Fig. 5. As expected, laser intensity and linewidth increase with increasing excitation.

Typical values of the collision cross section and duration are found [7(b)] to be 10^{-14} cm^2 and 10^{-12} s, respectively. For a perturber density of 10^{16} mole/cm^3 and active atom-perturber relative speed of 10^5 cm/s, the collision rate turns out to be $\Gamma\sim 10$ MHz at 1 Torr. This may be compared with the decay rates $\gamma_a\sim 10$ MHz and $\gamma_b\sim 50$ MHz for a He-Ne laser at 632.8 nm with the pressures of He (perturber) and Ne (active atom) being 1 Torr and 0.1 Torr, respectively. The Doppler width Ku is typically about 1.3 GHz.

VI. SUMMARY

In summary, we have presented a general theory of gas lasers taking into account both phase-interrupting and velocity-changing collisions between active atoms and perturber atoms. For simplicity, we have considered the case of a single-mode field in a unidirectional ring laser, but the results can be generalized very easily. The case of a standing-wave electric field in a two-mirror laser can be treated similarly by considering it as the sum of two oppositely directed running waves. Here exact analytical solutions in the strong-collision limit have been obtained and the laser intensity has been evaluated in the Doppler limit using the cavity self-consistency equation. The intensity can, of course, be calculated without the Doppler limit using (4.4). However, only for $v/(Ku)\sim 1$ appreciable deviation from the Doppler limit can be noticed. The "hole burning" in the steady-state population difference is shown to get washed out in the presence of VCC's. Also it is shown that the laser line shape cannot, in general, be written as a simple Voigt profile.

As is known [5], our results confirm that, in general, third-order perturbation theories provide accurate expressions for the mode amplitude near threshold, but overestimate the saturation and differ appreciably from the exact results for relative excitations as low as 1.1. For lasers operated far above threshold, one has to use the exact results given in Sec. V B, while the third-order perturbation-theory results (Section V A) are valid for low relative excitations.

ACKNOWLEDGMENT

A.A. acknowledges financial support from the University Grants Commission, India.

[1] P. R. Berman, in *New Trends in Atomic Physics,* edited by G. Grynberg and R. Stora (Elsevier Science, New York, 1984), pp. 451–514, and references therein.

[2] S. G. Rautian and I. I. Sobelman, Sov. Phys. Usp. **9**, 701 (1966).

[3] S. Singh and G. S. Agarwal, Phys. Rev. A **42**, 3070 (1990). Note that these authors have used the strong Doppler limit and hence their result for $\chi^{(3)}$ is independent of the detuning (Δ_l) of pump frequency from atomic resonance.

[4] (a) M. Sargent III, M. O. Scully, and W. E. Lamb, Jr., *Laser Physics* (Addison-Wesley, Reading, MA, 1977); (b) P. Meystre and M. Sargent III, *Elements of Quantum Optics* (Springer-Verlag, Berlin, 1990).

[5] S. Stenholm and W. E. Lamb, Jr., Phys. Rev. **181**, 618 (1969).

[6] (a) R. L. Fork and M. A. Pollack, Phys. Rev. **139A**, 1408 (1965); (b) P. W. Smith, J. Appl. Phys. **37**, 2089 (1966); (c) A. Szöke and A. Javan, Phys. Rev. **145**, 137 (1966).

[7] The opposite limit of $\Gamma_{ab}\gg Ku$ leads to motional narrowing; (a) R. H. Dicke, Phys. Rev. **89**, 472 (1953); (b) P. R. Berman, Appl. Phys. (Germany) **6**, 283 (1975).